Atmos. Chem. Phys. Discuss., 11, 29561–29600, 2011
www.atmos-chem-phys-discuss.net/11/29561/2011/
doi:10.5194/acpd-11-29561-2011
© Author(s) 2011. CC Attribution 3.0 License.

Atmospheric
Chemistry
and Physics
Discussions

This discussion paper is/has been under review for the journal Atmospheric Chemistry and Physics (ACP). Please refer to the corresponding final paper in ACP if available.

What do we learn on bromoform transport and chemistry in deep convection from fine scale modelling?

V. Marécal[1], M. Pirre[2], G. Krysztofiak[2], and B. Josse[1]

[1]Centre National de Recherches Météorologiques-Groupe d’étude de l’Atmosphère Météorologique, Météo-France and CNRS, URA1357, Toulouse, France
[2]Laboratoire de Physique et Chimie de l’Environnement et de l’Espace, CNRS and University of Orléans, UMR6115, Orléans France

Received: 29 June 2011 – Accepted: 19 October 2011 – Published: 2 November 2011

Correspondence to: V. Marécal (virginie.marecal@meteo.fr)

Published by Copernicus Publications on behalf of the European Geosciences Union.

Abstract

Bromoform is one of the main sources of halogenated Very Short-Lived Species (VSLS) that possibly contributes when degraded to the inorganic halogen loading in the stratosphere. Because of its short lifetime of about four weeks, its pathway to the stratosphere is mainly the transport by convection up to the tropical tropopause layer (TTL) and then by radiative ascent in the low stratosphere. Some of its degradation product gases (PGs) that are soluble can be scavenged and not reach the TTL.

In this paper we present a detailed modelling study of the transport and the degradation of bromoform and its PGs in convection. We use a 3-D-cloud resolving model coupled with a chemistry model including gaseous and aqueous chemistry. We run idealised simulations up to 10 days, initialised using a tropical radiosounding for atmospheric conditions and using outputs from a global chemistry-transport model for chemical species. Bromoform is initialised only in the low levels. The first simulation is run with stable atmospheric conditions. It shows that the sum of the bromoform and its PGs significantly decreases with time because of dry deposition and that PGs are mainly in the form of HBr after 2 days of simulation. The other simulation is similar to the first simulation but includes perturbations of temperature and of moisture leading to the development of a convective cloud reaching the TTL. Results of this simulation show an efficient vertical transport of the bromoform from the boundary layer in the upper troposphere and TTL (mixing ratio up to 45 % of the initial boundary layer mixing ratio). The organic PGs, which are for the most abundant of them not very soluble, are also uplifted efficiently. For the inorganic PGs, which are more abundant than organic PGs, their mixing ratios in the upper troposphere and in the TTL depend on the partitioning between inorganic soluble and inorganic non soluble species in the convective cloud. Important soluble species such as HBr and HOBr are efficiently scavenged by rain. This removal is reduced by the production of Br_2 (not soluble) in the gas phase from aqueous processes in the cloud droplets. This Br_2 production process is therefore important for the PG budget in the upper troposphere and in the TTL. We also showed

that this process is favoured by acidic conditions in the coud droplets, i.e. polluted conditions.

1 Introduction

Very short-lived halogenated substances (VSLSs) have been the focus of many studies recently because they likely contribute by degradation to the inorganic bromine loading in the stratosphere and consequently influence its ozone budget (WMO, 2007). The estimation of the part of the stratospheric inorganic bromine which comes from VSLS varies from <1 pptv up to >8 pptv, depending on the type of measurements (balloon-borne, e.g. Dorf et al., 2008; satellite, e.g. Sinnhuber et al., 2005) or of models used (e.g. Gettelman et al., 2009; Aschmann et al., 2009). The effect of VSLS source gases (SGs) and of their product gases (PGs) on the stratospheric bromine loading depends on their emissions, transport, chemistry, dry deposition and wash out. The chemical processing of SGs and PGs includes gaseous chemistry, photolysis, hydrolysis, aqueous chemistry and interactions with atmospheric ice particles.

The region of interest for VSLS is the tropics because VSLS are mainly emitted from the warm tropical oceans. Moreover, like other chemical species and aerosols, SGs and PGs mainly enter the stratosphere in the tropics. The main pathway is a rapid vertical transport by deep convection into the TTL (Tropical Tropopause Layer, see review paper by Fueglistaler et al., 2009) followed by a slow radiative ascent into the stratosphere for air having reached at least the level of zero radiative heating (LZRH, ~ 15.5 km altitude, 360 K). Deep convection is therefore a key process for the evolution of SGs and PGs in the troposphere before they possibly reach the stratosphere. Convection can lift within a few hours the emissions of SGs and the PGs from the boundary layer into the TTL. It can also influence the PGs budget through interactions between gaseous species and hydrometeors, in particular by the scavenging of soluble organic and inorganic PGs.

The model studies conducted so far on VSLSs are either based on 1-dimensional models (Gettelman et al., 2009), or on Lagrangian models (e.g. Brioude et al., 2010; Pisso et al., 2010; Schofield et al., 2011) or on 3-dimensional global models (e.g. Aschmann et al., 2009, 2011; Hossaini et al., 2010). They mainly seek at estimating the global impact of VSLSs on stratospheric halogen loading and ozone. Because of the large number and of the complexity of the processes involved in the VSLSs and PGs chemical processing, modelling studies generally use simplifications. Among the VSLSs, bromoform ($CHBr_3$) and dibromomethane (CH_2Br_2) are mostly studied because they are the most abundant (WMO report 2007). A detailed chemical scheme for degradation of $CHBr_3$ and CH_2Br_2 was proposed by Hossaini et al. (2010). They implemented this scheme in the 3-D TOMCAT/SLIMCAT global chemistry transport model. They showed that the organic PG abundance is small at the global scale. This indicates that SG degradation can reasonably be assumed to lead immediately to inorganic bromine. They estimated that $CHBr_3$ and CH_2Br_2 provide ~ 2.4 pptv of the inorganic bromine of the lower stratosphere with SG injection being the dominant pathway. Several recent studies showed the important role of deep convection on the halogen loading in the upper troposphere and lower stratosphere (Gettelman et al., 2009; Brioude et al., 2010; Hossaini et al., 2010; Pisso et al., 2010; Aschmann et al., 2011). 3-D-global models or Lagrangian models generally use on-line or off-line outputs fluxes from convection parameterizations to represent tracer transport by convection. But it is well known that there are large uncertainties on the tracer transport in deep convection parameterizations (e.g; Zhang et al., 2008; Arteta et al., 2009; Hoyle et al., 2011). The interactions between trace gases and hydrometeors (aqueous chemistry, hydrolysis, ice adsorption and associated washout) are usually represented in a simple manner in models using parameterized deep convection. For instance, Hossaini et al. (2010) assume that Br_y is removed in the troposphere by washout with a specified lifetime. This lifetime is a source of uncertainty in their calculations. In Aschmann et al. (2011), they improved the model by taking into account the heterogeneous activation reactions of dissolved/adsorbed bromine species on liquid aerosols, NAT (solid nitric acid trihydrate) and ice particles. They showed that there is very little removal of inorganic Br_y by ice sedimentation in the TTL.

Detailed studies at the fine scale are among the possible approaches to assess and to improve the assumptions used in global models on halogenated VSLS chemistry, in particular in deep convection parameterizations. In this context, the objective of the paper is to analyse at the local scale the impact of a tropical deep convective cloud on $CHBr_3$ and on its organic and inorganic PGs. Here we analyse results of cloud-resolving model simulations with on-line detailed gaseous and aqueous chemistry of bromoform for an idealized deep convective cloud. In particular we discuss a process that was not treated before: the Br_2 production in the gas phase from aqueous chemistry in the cloud droplets. The descriptions of the model and of the simulation setup are given in Sect. 2. The results are analysed in Sect. 3. Conclusions are given in Sect. 4.

2 Model description and simulation set-up

2.1 Meteorology: model and setup

The model used here is the 3-D-limited area model CATT-BRAMS (Coupled Aerosol Tracer Transport-Brazilian Regional Atmospheric Modeling system, Freitas et al., 2009) coupled on-line with a chemistry model. CATT-BRAMS is a numerical model designed to simulate atmospheric circulations at many scales. Here we use for our fine scale study a cloud-resolving configuration with a 1 km horizontal resolution and a 100 km × 100 km domain. We use 48 vertical levels spanning from the surface up to 24.5 km altitude. The vertical grid spacing is ~200 m in the boundary layer, 500 m in the free troposphere and in the tropical tropopause layer (up to 18 km altitude) and 1 km in the lower stratosphere. For this first study of $CHBr_3$ and PGs at the cloud scale, we chose a simple meteorological framework to represent the development of a deep convective cloud in the tropical atmosphere. At the initial time, the model meteorological variables (pressure, temperature and relative humidity) are assumed to be uniform horizontally. They are initialised vertically using a tropical radiosounding launched from Darwin (Australia, latitude = 12.1° S and longitude = 130.9° E) on 16 November 2005 at 23:00 UTC during the wet season in the frame of the SCOUT-O3 European Project (http://www.ozone-sec.ch.cam.ac.uk/scout_o3/). Note that Darwin is located in the Maritime Continent which is a region of high-reaching convection and concomitant exceptionally cold tropopause temperatures. It is also located close to a warm ocean coastal region where natural bromoform emissions are expected to be strong (e.g. Quack and Wallace, 2003). The radiosounding chosen corresponds to atmospheric stable conditions. We ran 2 simulations of 10-day duration which is approximately the lifetime of $CHBr_3$ in summer tropical conditions. The first one, called BG, is the background simulation corresponding to stable atmospheric conditions along the whole simulation. No cloud develops during the BG simulation. In the other simulation, called PERT hereafter, deep convection is forced to develop by adding perturbations of moisture and of temperature in the middle of the domain. The perturbation is applied to an area of 30 km radius. It is written:

$$\frac{drv}{dt} = \Delta rv_0 \cos^2\left(\frac{\pi d}{60}\right) \quad \text{and} \quad \frac{dT}{dt} = \Delta T_0 \cos^2\left(\frac{\pi d}{60}\right)$$

where d is the distance (km) from the centre of the perturbation, $\Delta rv_0 = 3.5 \times 10^{-3}\,\mathrm{g\,kg^{-1}\,s^{-1}}$ and $\Delta T_0 = 0.025\,\mathrm{K\,s^{-1}}$. This perturbation is applied during 800 s in the first 2 km of the atmosphere after 5 days and 6 h of simulation (14:00 LT). This allows the deep convective cloud to start developing in the afternoon as expected in the tropics. Cyclic boundary conditions are used. To represent microphysical processes we use the single-moment bulk parameterization proposed by Walko et al. (1995) in which seven types of hydrometeors are taken into account: cloud, rain, pristine ice, snow, aggregates, graupel and hail. The radiation scheme used is the radiative code of the Community Aerosol and Radiation Model for Atmospheres (CARMA, Toon et al., 1989) which takes into account the effect of hydrometeors and aerosols on radiation. Turbulent mixing is treated according to Mellor and Yamada (1982), which employs prognostic turbulent kinetic energy.

cc BY

2.2 Chemistry model

The chemistry model coupled on-line with the CATT-BRAMS includes gaseous chemistry, photolysis, $BrONO_2$ hydrolysis, aqueous chemistry of bromine species and dry deposition. As justified in Sect. 3.2, it does not include the interactions of the chemical species with the ice particles. The general chemical system of equations used is:

$$\frac{dX_\mathrm{g}}{dt} = -k_{X_\mathrm{C}} V_\mathrm{C} X_\mathrm{g} - k_{X_\mathrm{R}} V_\mathrm{R} X_\mathrm{g} + \frac{k_{X_\mathrm{C}} X_\mathrm{C}}{RTH_X} + \frac{k_{X_\mathrm{R}} X_\mathrm{R}}{RTH_X} - D_{X_\mathrm{dep}} + P_{X_\mathrm{g}} - L_{X_\mathrm{g}} X_\mathrm{g} \tag{1}$$

$$\frac{dXc}{dt} = k_{X_\mathrm{C}} V_\mathrm{C} X_\mathrm{g} - \frac{k_{X_\mathrm{C}} X_\mathrm{C}}{RTH_X} + P_{X_\mathrm{C}} - L_{X_\mathrm{C}} X_\mathrm{C} \tag{2}$$

$$\frac{dX_\mathrm{R}}{dt} = k_{X_\mathrm{R}} V_\mathrm{R} X_\mathrm{g} - \frac{k_{X_\mathrm{R}} X_\mathrm{R}}{RTH_X} + P_{X_\mathrm{R}} - L_{X_\mathrm{R}} X_\mathrm{R} \tag{3}$$

where

- X_g is the concentration of species X in the gas phase in molecules per cm^3 of air,
- X_C (resp. X_R) is the concentration of species X in the cloud droplets (resp. raindrops) in molecules per $\mathrm{cm}^3$of air,
- V_C and V_R are the volume densities of cloud and of rain in m^3 water/m^3 air computed from their mass mixing ratios,
- k_{X_C} (resp. k_{X_R}) in s^{-1} is the mass transfer between the gas and the cloud droplets (resp. raindrops) of species X,
- H_X is the effective Henry's constant of species X in $\mathrm{mol\,l^{-1}\,atm^{-1}}$,
- R is the universal gas constant in $\mathrm{l\,atm\,mol^{-1}\,K^{-1}}$,
- T is the temperature in K,

- P_{X_C} term (resp. P_{X_R} terms) is the production term in the cloud droplets (resp. raindrops) of species X,
- L_{X_C} (resp. L_{X_R}) is the loss term of species X in the cloud droplets (resp. raindrops),
- P_{X_g} and L_{X_g} terms are the production and loss terms of species X in the gas phase including also hydrolysis,
- D_{X_dep} term is the dry deposition of species X at the lowest model level.

In the case of non soluble species only Eq. (1) is solved and only the last two terms of Eq. (1) are taken into account.

The gaseous chemistry model includes the chemistry for CO, CH_4, O_3, NO_y, HO_x (Barth et al., 2007), Br_y, and organic chemistry of the degradation of $CHBr_3$ (Hossaini et al., 2010). Cl_y and NMHC chemistry is not included to save computing time. For Cl_y this is justified because there is only a small expected impact on the degradation of $CHBr_3$ and PG chemistry because chlorine atoms are only involved in the lifetime of $CHBr_3$ which is mainly driven by OH oxidation and photolysis (WMO, 2007). Moreover the heterogeneous reaction HBr + HOCl (IUPAC subcommittee on Gas Kinetic Data evaluation VI.12.8) is slower by about a factor 10^4 than HBr + HOCl (Fickert et al., 1999). The lack of NMHC chemistry can significantly affect HO_x precursors and therefore HO_x concentrations, but mainly in the upper troposphere (Jaeglé et al., 2001). In our study gaseous chemistry is only important in the lower troposphere. For $CHBr_3$ the reactions in gas phase proposed in Hossaini et al. (2010) are used. The rate constants of the organic chemistry of $CHBr_3$ are from Hossaini et al. (2010). Other gaseous rate constants cross-sections are from JPL (2007) and IUPAC (IUPAC Subcommittee on Gas Kinetic Data Evaluation, http://www.iupac-kinetic.ch.cam.ac.uk). Photolysis rates are computed on-line using Fast-TUV model (Tie et al., 2003) in order to take into account the effect of clouds on photolysis rates in an interactive way. The photolysis cross-sections are from JPL (2007) and IUPAC.

CC BY

The model includes the hydrolysis reaction of $BrONO_2$ on the cloud droplets and raindrops leading to the formation of HOBr:

$$BrONO_2 + H_2O \rightarrow HOBr + HNO_3 \tag{R1}$$

The rate constant k_{1C} (resp. k_{1R}) of Eq. (R1) on the cloud droplets (resp. the raindrops) is computed using the mean mixing ratio and the mean-mass radius of cloud droplets (resp. raindrops) from the bulk-microphysical scheme. Following Yang et al. (2005) they are written:

$$k_{1C} = \frac{V_C}{\left(\frac{r_C^2}{3D_g} + \frac{4r_C}{3v\gamma}\right)} \quad \text{and} \quad k_{1R} = \frac{V_R}{\left(\frac{r_R^2}{3D_g} + \frac{4r_R}{3v\gamma}\right)} \tag{4}$$

where

- r_C (resp. r_R) is the mean-mass radius of the cloud (resp. rain) size distribution. r_C is computed by the microphysical scheme of the model and depends on the grid point and on time. It is typically 10 µm. r_R is fixed to 250 µm in the microphysical scheme.

- v is the thermal velocity of $BrONO_2$,

- D_g is the gas phase diffusivity of $BrONO_2$ in air: $D_g = \lambda v/3$ where λ is mean free path which is assumed to be $\lambda = 0.1$ µm (Sander and Crutzen, 1996),

- γ is the accommodation coefficient. It is assumed to be: $\gamma = 0.3$ (Yang et al., 2005).

The model takes into account the effect on chemical species of condensation, water vapour deposition, evaporation and sedimentation, these microphysical processes being estimated by the bulk microphysical scheme. It also includes the reversible kinetic transfer of species from the gas phase to the cloud droplets and raindrops (controlled by the effective Henry's and accommodation constants) and the transfer of species from cloud droplets to raindrops during the coalescence process and to the ice particles during the riming process. The retention coefficient used in the transfer from cloud to ice particles is assumed to be equal to 1 for all species. Once in the ice particles, the chemical species are assumed to be lost by wash out. This last assumption is realistic because the ice particles mainly grow by riming in the simulation and form fast-falling graupel and hail particles. Some of them could nevertheless be transported by convection up to the TTL where they could evaporate, releasing chemical species in the gas phase. Taking into account this process would need to follow numerically the concentration of the chemical species in the five ice categories of the microphysical scheme. It has not been taken into account in the simulation to save computing time.

The Henry's constants used in the model are mainly from Sander (1999). Table 1 gives the Henry's constants for the bromine species. The values from Yang et al. (2005) are used for HBr and Br_2. For the hydroperoxydes and aldehydes, and ketone organic bromine product gases we use those computed in Krysztofiak et al. (2011). In this paper, the Henry's constants are estimated by the Bond contribution method (BCM) (Meylan and Howard, 1991) and by the Molecular connectivity index (MCI) method (Nirmalakhandan and Speece, 1988). Krysztofiak et al. (2011, Supplement) show that the MCI method is better to estimate the Henry's law constant for aldehyde and ketone whereas both methods agree on the estimation of the constant for hydroperoxide compounds. The temperature dependencies are derived from CH_3OOH for hydroperoxyde compounds and from RCHO and RR'CO for aldehyde and ketone, respectively (Sander et al., 1999). The accommodation coefficients are derived from those used in Barth et al. (2001).

The mass transfer between the gas and the liquid droplets takes into account the diffusion in the gas phase and across the droplets interface. Like in many atmospheric chemistry models (e.g. Barth et al., 2003) the diffusion inside cloud and rain droplets is assumed not to be rate limited, meaning that the species are well mixed within the droplets. The mass transfer coefficients k_{X_C} and k_{X_R} are then written:

$$k_{X_\mathrm{C}} = \frac{1}{\left(\frac{r_\mathrm{C}^2}{3D_{\mathrm{g}X}} + \frac{4r_\mathrm{C}}{3v_X\alpha_X}\right)} \qquad k_{X_\mathrm{R}} = \frac{1}{\left(\frac{r_\mathrm{R}^2}{3D_{\mathrm{g}X}} + \frac{4r_\mathrm{R}}{3v_X\alpha_X}\right)} \tag{5}$$

where v_X is the thermal velocity, $D_{\mathrm{g}X}$ the diffusion coefficient in air and α_X the accommodation coefficient of species X. The mass transfer coefficient for cloud is typically $k_{X_\mathrm{C}} = 2 \times 10^5\,\mathrm{s}^{-1}$. It is $k_{X_\mathrm{R}} = 5 \times 10^2\,\mathrm{s}^{-1}$ for rain.

The model also takes into account the following reactions of Bry species in the aqueous phase:

$$\mathrm{HOBr_{aq} + Br^- + H^+ \rightarrow Br_{2aq} + H_2O} \tag{R2}$$

$$\mathrm{Br_{2aq}(+H_2O) \rightarrow HOBr_{aq} + Br^- + H^+} \tag{R3}$$

The rate constants of these reactions are, respectively (Fickert et al., 1999): $k_2 = 1.6 \times 10^{10}\,\mathrm{mol^{-2}\,l^2\,s^{-1}}$, $k_3 = 110\,\mathrm{s}^{-1}$. In the literature, Reaction (R2) is taken into account in sulphate aerosols and/or in sea salt aerosols (von Glasow and Crutzen, 2007). Here we use Reaction (R2) in liquid hydrometeors instead of aerosols. Although Reaction (R3) exists, it has been neglected so far in atmospheric chemistry models. This is because $\mathrm{Br_2}$ has a very low solubility leading to a very small time of residence in small particles such as sulphate and sea salt aerosols. In this case $\mathrm{Br_2}$ is very rapidly released to the gas phase before Reaction (R3) can take place. Since cloud droplets and raindrops have larger radius than aerosols, the time of residence of $\mathrm{Br_2}$ in these droplets is larger. In this case Reaction (R3) has time to take place and must be taken into account. As shown in Appendix A, the residence time of $\mathrm{Br_2}$ in the cloud droplets ($\sim 3 \times 10^{-4}$ s) is nevertheless smaller than the characteristic time of Reaction (R3) (9×10^{-3} s) leading to a significant release of $\mathrm{Br_2}$ in the gas phase from cloud droplets similarly to aerosols. On the contrary, the residence time of $\mathrm{Br_2}$ in the raindrops (~ 0.1 s) is larger than the characteristic time of Reaction (R3) leading to a weak release of $\mathrm{Br_2}$ in the gas phase. For this reason, in this paper, the release of $\mathrm{Br_2}$ by aqueous reactions in raindrops is neglected relatively to the release by aqueous reactions in cloud droplets. For the cloud, Henry's equilibrium between the gas and the aqueous phases of Br_2 may be assumed and Reactions (R2) and (R3) can be then written in the condensed form:

$$\mathrm{HOBr_C} + \mathrm{Br_C^-} \rightarrow \mathrm{Br_{2g}} \quad \text{with the rate constant } k_4 = k_2[\mathrm{H^+}]/(6.02 \times 10^{20} V_\mathrm{C}) \tag{R4}$$

$$\mathrm{Br_{2g}} \rightarrow \mathrm{HOBr_C} + \mathrm{Br_C^-} \quad \text{with the rate constant } k_5 = k_3 \times \mathrm{H_{Br_2}} RTV_\mathrm{C} \tag{R5}$$

where $HOBr_C$ and Br_C^- represent the molecules of HOBr and the Br ions from HBr in the clouds per cm^3 of air. Note that k_4 depends on the pH of the cloud droplets.

For HBr and HOBr the Henry's equilibrium cannot be assumed. Therefore aqueous chemistry Eqs. (2) and (3) are solved similarly to the gaseous chemistry Eq. (1). Equations (1)–(3) are solved simultaneously with the chemical solver Rosenbrock RODAS3 (Sandu et al., 1997).

The dry deposition is taken into account for soluble species, in particular for HBr, HOBr and soluble bromine organic species. The dry deposition velocity is computed using the surface resistance defined by Wesely (1989).

2.3 Chemistry initialisation

The initialisation is the same for the BG and PERT simulations. At the beginning of the simulations, CO, O_3 and CH_4 are assumed to be uniform horizontally and fixed vertically to the averaged profiles computed by the global Chemistry Transport Model MOCAGE (Josse et al., 2004; Bousserez et al., 2007) at the grid point closest to Darwin (12° S, 131° W) for the whole November 2005 month. The MOCAGE simulation has a 2° × 2° horizontal resolution and uses the RACM scheme for tropospheric chemistry (Stockwell et al., 1997) and the REPROBUS scheme for stratospheric chemistry (Lefèvre et al., 1994). The chemical composition of the profile selected is typical of moderately polluted conditions. Since HNO_3 is the most abundant NO_y, HNO_3 is initialised with the MOCAGE mean profile of NO_y and other NO_y species are set to zero.

Bromoform is assumed to decrease from the surface to the upper levels with the maximum mixing ratios located in the first 1 km (approximate depth of the boundary layer). A mixing ratio of 40 pptv is assumed at the surface. It corresponds to the value measured close to the sources by Yokouchi et al. (2005). Figure 1 shows the initial profile of the $CHBr_3$ mixing ratio. All other species are set to zero initially, including inorganic and organic bromine product gases. No emissions are assumed during the BG and PERT simulations. The simulation represents therefore the evolution of an air mass initially rich in bromoform. Note that the dry deposition is the only loss mechanism for Br_y species in the BG simulation because this simulation corresponds to stable and cloud/rain free conditions.

3 Results

3.1 The BG simulation

The time step for the dynamics of the BG simulation is 30 s. The maximum chemical time step is 180 s. It is reduced, when needed, to increase the accuracy of the calculations. Photolysis coefficients are computed on-line every 300 s. The BG simulation is run from 16 May 23:00 UTC until 26 May 23:00 UTC. This duration of 10 days corresponds approximately to the lifetime of the bromoform at the latitude and the season of the simulation. Since this is the number of bromine atoms reaching the TTL which is of interest, all mixing ratios of bromine species are weighted hereafter by their number of bromine atoms. For instance, the mixing ratio of $CHBr_3$ will refer to 3 times the actual $CHBr_3$ mixing ratio.

Figure 2 shows the evolution of the bromoform and of its product gases at the altitude of 1 km at the middle point of the domain. The decrease of $CHBr_3$ is mainly due to photolysis and to the reaction with OH. Photolysis is more efficient than the reaction with OH as shown in Table 2. The computed lifetime at 1 km altitude is 9.1 days (Table 2). This lifetime is smaller than the global mean lifetime of bromoform which is 26 days (WMO, 2007). This is due to the low ozone column prevailing at the location of the simulation and to the large concentration of OH (Table 2). The decrease of $CHBr_3$ is also due to the vertical diffusion. Table 2 gives also the mean values over the 10-day simulation, at 1 km altitude, of OH, HO_2, NO_x and O_3. The simulation corresponds to a low NO_x regime which explains the low value of O_3.

The mixing ratios of PGs increase as $CHBr_3$ mixing ratio decreases (Fig. 2). The sum of both $CHBr_3$ and PGs mixing ratios decreases with time. This is mainly due to their loss by dry deposition and also to diffusion. Figure 2 also shows that the bromoform and the PGs are of the same order of magnitude during the second part of the simulation.

Product gases (Fig. 3) are mainly in the form HBr which is the final product of the degradation of bromoform. The increase of HBr mixing ratio is nevertheless limited by dry deposition. After 5 days of simulation HBr mixing ratio is between 2 and 3 times larger than the organic product gases and 5 times larger than the other inorganic product gases. Among the organic product gases the most abundant is CBr_2O (maximum: 7 pptv of bromine atoms). CBr_3OOH, $CHBr_2OOH$ and CHBrO are of the same order of magnitude (maximum ~ 2 pptv of bromine atoms each) while CBr_3O_2 and $CHBr_2O_2$ have very low concentrations. Note that CBr_3OOH and $CHBr_2OOH$ are highly soluble while CBr_2O and CHBrO have low solubilities.

3.2 The PERT simulation

In this simulation the dynamical time step is 4 s and the maximum chemical step is 12 s. Photolysis rates are computed every 100 s. The temperature and moisture perturbations are applied after 5 days and 6 h of simulation. The starting time of the perturbation is noted t_0 hereafter. At t_0, the mixing ratio of bromoform is of the same order as the mixing ratio of the product gases in the low levels (Fig. 2). Figure 4 presents vertical cross-sections in the middle of the convective cloud at different times. Twenty minutes after the starting time of the perturbation (t_0 + 20 min) convection reaches 13 km altitude with total condensed droplets (liquid + ice), rain and liquid cloud mixing ratios up to 16, 8 and 3.3 g kg^{-1}, respectively. At $t_0 + 30$ min convection is fully developed with a maximum altitude of ~ 17 km, i.e. within the TTL. At this time, the maximum rain mixing ratio is 15 g kg^{-1} while liquid cloud mixing ratios are lower than 0.5 g kg^{-1}. Above 6 km, the condensed phase is only composed of ice particles with mixing ratios up to 5 g kg^{-1}. The rain and the liquid cloud totally disappear after $t_0 + 110$ min while ice particles remain present at high altitude after $t_0 + 2$ h.

We firstly study the evolution of the $CHBr_3$ source gas. It is transported rapidly upward when deep convection develops as illustrated by Fig. 5 showing the vertical cross-section of the mixing ratio of $CHBr_3$ at $t_0 + 30$ min. Its maximum value is ~ 55 pptv at 13.5 km altitude. The turbulent mixing of the chemical species is taken into in the model leading to the dilution of $CHBr_3$ during convection, mainly at the edges. Nevertheless the comparison with values close to surface (~ 70 pptv) shows that a significant part of $CHBr_3$ is transported into the upper troposphere and TTL. Because of its very low Henry's constant $CHBr_3$ is hardly washed out by convective rain.

The mixing ratios of the organic product gases in the upper troposphere and TTL largely depend on their Henry's constants (see Table 1). Examples of the results for two important organic PGs (CBr_3OOH and CBr_2O) at $t_0 + 30$ min are shown in Fig. 6. The mixing ratio of CBr_3OOH is negligible in the TTL because it is washed out by rain (Fig. 6a). Among organic PGs, CBr_2O has the highest mixing ratio in the upper troposphere and TTL with a maximum of ~ 7 pptv (Fig. 6b). This is because it is largely produced by gaseous chemistry and hardly washed out thanks to its low Henry's constant.

The analysis of the inorganic species is more complex since they undergo not only gaseous chemistry and wash out but also hydrolysis and aqueous chemistry. Rapidly after cloud and rain formation, the hydrolysis leads to a severe loss of $BrONO_2$ which feeds HOBr. Simultaneously most of HOBr and HBr is dissolved in rain and then scavenged. Figure 7 shows the vertical cross-section of HBr at the maximum of the convection development. Very low mixing ratios of HBr (less than 0.1 ptv) are found in the upper troposphere. This justifies not taking into account in this simulation the reactions with the ice particles present in the upper troposphere since the main reactions on ice are between inorganic bromine species and HBr adsorbed on the ice surfaces (Aschmann et al., 2011). Part of HBr and HOBr is also dissolved in the cloud droplets where they undergo Reaction (R4) and form Br_2 in the gas phase. This gaseous Br_2 rapidly forms Br, BrO and HOBr in sunlight conditions. The formation efficiency for Br_2 depends on the pH of the cloud droplets. This is illustrated in Fig. 8 showing the cross-sections of Br_x ($Br + 2Br_2 + BrO + HOBr$) in the gas phase at $t_0 + 20$ min for pH = 5 and pH = 4. The pH = 5 case corresponds to standard atmospheric conditions while pH = 4 represents more polluted acidic conditions. With pH = 4 there is more gaseous Br_x produced because Reaction (R4) is more efficient. Br_x is mainly formed at the edge of the cloud since the sunlight is reduced deep inside the cloud. The Br_x formation at the edge of the cloud is similar to the so-called "bromine explosion" observed in presence of sea salt aerosols (Barrie et al., 1988) and aerosols in volcanic plumes (Bobrowski et al., 2007; Roberts et al., 2009). Figure 9 shows the cross-section of Br_x at the mature stage of the convective cloud ($t_0 + 30$ min) for both pH = 5 and pH = 4. At this time, Br_x has reached the TTL with higher mixing ratios for pH = 4 (max ~ 8 pptv) than for pH = 5 (max ~ 3 pptv), similarly to $t_0 + 20$ min. The largest mixing ratios remain in the low and mid troposphere because Br_x is mainly formed at the edge of the liquid cloud where lower vertical ascent velocities are simulated compared to the ascent velocities in the middle of convection.

Figure 10 shows the vertical cross-sections of $CHBr_3$ and of the total PGs in the PERT simulation compared with the BG simulation at the end of the convective event ($t_0 + 110$ min). The impact of convection on the chemical composition of the lower troposphere below 2000 m altitude is relatively small. It is more important on the PGs because of the wash out of the soluble species. $CHBr_3$ and PGs which have been lifted by the vertical winds in the convection tower remain in the upper troposphere at the end of the convective event. $CHBr_3$ and PGs mixing ratios maxima are 40 and 7 pptv, respectively at ~ 12 km altitude (see Figs. 10b,d). They are lower than at $t_0 + 30$ min, time of the maximum of the convective development.

To analyse in more detail the final effect of the convective event we plotted in Fig. 11 the mean profiles averaged horizontally over the whole domain of the organic PGs, inorganic PGs and total PGs mixing ratios relative to $CHBr_3$ mixing ratio at the end of the convective event ($t_0 + 110$ min). Figure 11a–c is, respectively for the simulation with cloud pH = 5, with cloud pH = 4 and without bromine species aqueous reactions in the cloud. The total PGs relative to $CHBr_3$ for the simulation assuming pH = 5 (Fig. 11a) is large up to 5 km altitude, reaching a maximum of 90 % around 3 km altitude.

In 0–5 km layer the three simulations are different since this layer corresponds to where rain is mainly present. In acidic conditions (pH = 4), HBr in the rain is less washed out than in cleaner conditions (pH=5) because of the formation of Br_2 in the cloud. Without bromine species aqueous reactions in the cloud, the total PGs to $CHBr_3$ ratio is lower because of no gaseous Br_2 production. Above 5 km altitude, the species present are those which were transported by convection. The ratio of organic PGs relative to $CHBr_3$ for the three simulations vary similarly from 18 % at 5 km altitude to 14 % at 18 km altitude. The contribution of the organic PGs in the upper troposphere and TTL is therefore significant. The lack of difference between the three simulations is because aqueous chemistry in cloud does not influence $CHBr_3$ and organic PGs because of their low solubility. In the convective conditions chosen in the PERT simulation the contribution of organic PGs is significant and larger than the inorganic PGs contribution. Hossaini et al. (2010) in their detailed study of $CHBr_3$ degradation found an average value of ~3 % at 100 hPa (~16 km) at tropical latitudes. The difference with our simulations is likely due to the high sunlight conditions of our simulations. Relatively to mean conditions, such extreme conditions lead to decrease more the lifetime of $CHBr_3$ than the lifetime of the final organic product gases CBr_2O and CHBrO. Above 5 km altitude the variations of the total PGs to $CHBr_3$ ratio follow the variations of the inorganic species ratio. For the simulation assuming pH = 5 (Fig. 11a), the inorganic PGs to $CHBr_3$ ratio decreases from 15 % to 3 % with increasing altitude with the total PGs to $CHBr_3$ ratio decreasing from 33 % to 17 %. Therefore the amount of the total PGs relative to $CHBr_3$ brought into the upper troposphere and TTL by convection is

cc BY

significant. It is larger than in the simulation without bromine species aqueous reactions in the cloud (25 % to 16 %) because in the pH = 5 simulation there is production of Br_x which is transported in the upper troposphere and the TTL. In the pH = 4 simulation the inorganic PGs to $CHBr_3$ ratio is larger (from 30 % to 7 %) than in the pH = 5 simulation because of the enhanced production of Br_x. The total PGs to $CHBr_3$ ratio for pH = 4 varies from 48 % to 21 %.

These results indicate that convection transports efficiently organic PGs, which are for the more abundant of them not very soluble, and that inorganic PGs are not fully scavenged if the aqueous chemistry in cloud droplets is taken into account. This last process depends on the cloud pH.

4 Conclusions

Bromoform is known to be one of the main sources of halogenated VSLSs that could influence the bromine loading in the stratosphere. Tropical convection is the main pathway for bromoform and its product gases (PGs) to the tropical tropopause layer (TTL). From the TTL they can enter the stratosphere via radiative ascent. In this paper we present a detailed study of the transport and degradation of the bromoform and its PGs in convective conditions at the cloud scale. The objective is to evaluate the relative importance of the different processes affecting the spatial distribution of bromoform and its product gases in convective conditions, in particular the interactions of PGs with the liquid cloud and rain. We use the three-dimensional cloud resolving model with tracer transport CATT-BRAMS coupled on-line with a chemistry model. The chemistry model includes gaseous chemistry, photolysis, $BrONO_2$ hydrolysis, aqueous chemistry of bromine species and dry deposition. This model is more detailed than what is used in current global models. In particular we take into account the aqueous chemistry including the production of Br_2 in the gas phase via the reactions in the aqueous phase.

For this study at the convective scale, we used idealized meteorological conditions from a tropical radiosounding launched during the convective season in North Australia. Two simulations were done. The BG (background) simulation corresponds to stable atmospheric conditions and was run for 10 days. The PERT simulation is similar to the BG simulation except that temperature and moisture perturbations were applied in the lowest 2 km layer after 5 days and 6 h leading to the development of a convective cloud reaching the TTL. The results of the BG simulation show that bromoform mixing ratio in the boundary layer decreases and PGs increase with time. Product gases are mainly in the form of HBr and organic products. Because of dry deposition the sum of bromoform and PGs decreases with time. In the PERT simulation a significant proportion of $CHBr_3$ is transported by convection into the upper troposphere and the TTL because it is not a soluble species. Organic species, which are for the most abundant of them not very soluble, are also efficiently lifted in the TTL. The quantity of inorganic PGs reaching the upper troposphere and the TTL depends tightly on the interactions between the gas phase and the aqueous phase. The results clearly show that one important process in the partitioning of inorganic PGs between soluble and non-soluble species is the formation of Br_2 in the gas phase released from cloud droplets containing dissolved HOBr and HBr. This reaction favours the formation of non soluble inorganic PGs and reduces HBr and HOBr scavenging leading to an increase of non-soluble inorganic mixing ratios in the upper troposphere and in the TTL. This process depends on the cloud droplet acidity and is significantly more efficient in polluted conditions (high acidity).

In this study the chemical model we developed is based on the current atmospheric chemistry knowledge. There are several sources of uncertainties in this model. Firstly, the results depend strongly on the Henry's constants for inorganic PGs which were determined here theoretically by Krystofiak et al. (2011). They need to be confirmed by experimental measurements. Secondly, the simulations were run in idealised convective conditions. In real conditions, several parameters could be different from those used in the PERT simulation. This could lead to a different proportion of PGs (organic and inorganic) lifted by convection in the TTL. The differences between idealised and real conditions that are expected to lead to significant differences in the results are:

- the relative concentrations of organic and inorganic PGs with respect to $CHBr_3$ before convection starts,
- the concentrations of soluble and low solubility organic and inorganic PGs before convection starts,
- the mixing ratios of liquid cloud and rain produced by convection,
- the pH of liquid cloud particles.

To go a step further, simulations of real case studies are required. This will be possible in the frame of the SHIVA European project. One objective of this project is the understanding of the chemistry and pathways to the stratosphere of halogenated VSLSs. The SHIVA field campaign will provide validation data for model simulations. Once validated on real case studies, the results on the partitioning between $CHBr_3$, organic and inorganic PGs reaching the TTL could be taken into account in global models via parameterizations.

Two issues which have not been discussed in the paper are the transport of species transferred from cloud to ice particles during the riming process and the interaction between PGs in the gas phase and the ice particles in the atmosphere. Most of the species transferred by riming in the ice phase are rapidly washed out because most rimed particles are dense and therefore fast-falling. But the small proportion of species which are transferred by riming to small slow-falling ice particles could be transported to the TTL and possibly released to the gas phase by sublimation. This could be taken into account in a future work. The interaction between PGs and ice particles has not been included in our chemistry model although it was taken into account by Aschmann et al. (2011) in their simulations at the global scale. For our study of bromoform at the local scale, this process is likely not very important since only very small amounts of HBr reach altitude levels where dry ice particles grow by water deposition. This is because HBr is efficiently scavenged by cloud and rain below and cannot therefore be transported in the upper troposphere where ice is present. Nevertheless, this process is likely important several hours after convective events in the cirrus layer that generally remains after convection. At this cloud stage HBr can be produced from inorganic PGs transported by convection into the upper troposphere and the TTL and interact with ice particles.

Appendix A

Production of Br_2 in the gas phase via the reactions in the aqueous phase

For Br_2, Eqs. (1)–(3) can be written:

$$\frac{d[\mathrm{Br_2}]_\mathrm{g}}{dt} = \frac{k_\mathrm{C}}{HRT}[\mathrm{Br_2}]_\mathrm{C} - k_\mathrm{C}V_\mathrm{C}[\mathrm{Br_2}]_\mathrm{g} + \frac{k_\mathrm{R}}{HRT}[\mathrm{Br_2}]_\mathrm{R} - k_\mathrm{R}V_\mathrm{R}[\mathrm{Br_2}]_\mathrm{g} + P_\mathrm{g} - L_\mathrm{g}[\mathrm{Br_2}]_\mathrm{g} \tag{A1}$$

$$\frac{d[\mathrm{Br_2}]_\mathrm{C}}{dt} = k_2[\mathrm{Br^-}]_\mathrm{C}[\mathrm{H^+}]_\mathrm{C}[\mathrm{HOBr}]_\mathrm{C} - k_3[\mathrm{Br_2}]_\mathrm{C} - \frac{k_\mathrm{C}}{HRT}[\mathrm{Br_2}]_\mathrm{C} + k_\mathrm{C}V_\mathrm{C}[\mathrm{Br_2}]_\mathrm{g} \tag{A2}$$

$$\frac{d[\mathrm{Br_2}]_\mathrm{R}}{dt} = k_2[\mathrm{Br^-}]_\mathrm{R}[\mathrm{H^+}]_\mathrm{R}[\mathrm{HOBr}]_\mathrm{R} - k_3[\mathrm{Br_2}]_\mathrm{R} - \frac{k_\mathrm{R}}{HRT}[\mathrm{Br_2}]_\mathrm{R} + k_\mathrm{R}V_\mathrm{R}[\mathrm{Br_2}]_\mathrm{g} \tag{A3}$$

where $[\mathrm{Br_2}]_\mathrm{C}$, $[\mathrm{Br_2}]_\mathrm{R}$, $[\mathrm{HOBr}]_\mathrm{C}$ $[\mathrm{HOBr}]_\mathrm{R}$ are the concentrations per cm^3 of air of Br_2 and HOBr in cloud droplets and raindrops, $[\mathrm{Br_2}]_\mathrm{g}$ is the concentration of Br_2 in the gas phase, $[\mathrm{Br^-}]_\mathrm{C}$, $[\mathrm{Br^-}]_\mathrm{R}$, $[\mathrm{H^+}]_\mathrm{C}$ and $[\mathrm{H^+}]_\mathrm{R}$ are the concentrations (in mol per l of water) of bromine ions and pH in the cloud or the rain droplets, k_C and k_R are the mass transfer coefficients of Br_2 in cloud and rain, respectively, H is the Br_2 Henry's coefficient, P_g and L_g are the production and loss term of Br_2 in the gas phase, V_C, V_R, k_2 and k_3 are defined in Sect. 2.2.

Since the loss terms of Eqs. (A2) and (A3) are very large, the equilibrium is reached rapidly leading to:

$$\left(k_3+\frac{k_\mathrm{C}}{HRT}\right)[\mathrm{Br_2}]_\mathrm{C}=k_2[\mathrm{Br}^-]_\mathrm{C}[\mathrm{H}^+]_\mathrm{C}[\mathrm{HOBr}]_\mathrm{C}+k_\mathrm{C}V_\mathrm{C}[\mathrm{Br_2}]_\mathrm{g} \tag{A4}$$

$$\left(k_3+\frac{k_\mathrm{R}}{HRT}\right)[\mathrm{Br_2}]_\mathrm{R}=k_2[\mathrm{Br}^-]_\mathrm{R}[\mathrm{H}^+]_\mathrm{R}[\mathrm{HOBr}]_\mathrm{R}+k_\mathrm{R}V_\mathrm{R}[\mathrm{Br_2}]_\mathrm{g} \tag{A5}$$

For $\mathrm{Br_2}$, the sum of Eqs. (A1), (A2) and (A4) leads to:

$$\begin{aligned}\frac{d[\mathrm{Br_2}]_T}{dt} &= k_2[\mathrm{Br}^-]_\mathrm{C}[\mathrm{H}^+]_\mathrm{C}[\mathrm{HOBr}]_\mathrm{C}+k_2[\mathrm{Br}^-]_\mathrm{R}[\mathrm{H}^+]_\mathrm{R}[\mathrm{HOBr}]_\mathrm{R}-k_3[\mathrm{Br_2}]_\mathrm{C}\\ &\quad -k_3[\mathrm{Br_2}]_\mathrm{R}+P_\mathrm{G}-L_\mathrm{G}[\mathrm{Br_2}]_\mathrm{g}\end{aligned} \tag{A6}$$

where $[\mathrm{Br_2}]_T=[\mathrm{Br_2}]_\mathrm{g}+[\mathrm{Br_2}]_\mathrm{C}+[\mathrm{Br_2}]_\mathrm{R}$.

Using Eqs. (A4) and (A5) and assuming $\frac{k_\mathrm{C}}{HRT}\gg k_3\gg\frac{k_\mathrm{R}}{HRT}$ as discussed in Sect. 2.2, Eq. (A6) can be written:

$$\begin{aligned}\frac{d[\mathrm{Br_2}]_T}{dt} &= k_2[\mathrm{Br}^-]_\mathrm{C}[\mathrm{H}^+]_\mathrm{C}[\mathrm{HOBr}]_\mathrm{C}+k_2\frac{k_\mathrm{R}}{k_3HRT}[\mathrm{Br}^-]_\mathrm{R}[\mathrm{H}^+]_\mathrm{R}[\mathrm{HOBr}]_\mathrm{R}-k_3HRTV_\mathrm{C}[\mathrm{Br_2}]_\mathrm{g}\\ &\quad -k_\mathrm{R}V_\mathrm{R}[\mathrm{Br_2}]_\mathrm{g}+P_\mathrm{G}-L_\mathrm{G}[\mathrm{Br_2}]_\mathrm{g}\end{aligned} \tag{A7}$$

If the concentrations of Br^- and HOBr were equal in the cloud and in the rain and if the volume of the rain and cloud were also equal, the second term and the fourth term, which are relative to the rain, would approximately be 10 times lower than the first and the third terms, which are relative to clouds. In the simulations, the concentrations of bromine ions (Br^-) and HOBr in the cloud compared with those in the rain are varying as a function of the grid point and of the time. Cloud and rain volumes are also varying. Nevertheless, at the beginning of the formation of the convective event, i.e. approximately from t_0+15 min to t_0+25 min (t_0 is defined in Sect. 3.2), they are of the same order on average. It is in this time interval that $\mathrm{Br_2}$ is produced. It is then possible to neglect the second and fourth terms of Eq. (A7).

Moreover the concentration of Br_2 in the gas phase is well larger than the concentration in aqueous phase. For these reasons, Eq. (A7) can be written in the simplified final form:

$$\frac{d[\mathrm{Br_2}]_\mathrm{g}}{dt} = k_2[\mathrm{Br^-}]_\mathrm{C}[\mathrm{H^+}]_\mathrm{C}[\mathrm{HOBr}]_\mathrm{C} - k_3 HRTV_\mathrm{C}[\mathrm{Br_2}]_\mathrm{g} + P_\mathrm{G} - L_\mathrm{G}[\mathrm{Br_2}]_\mathrm{g} \qquad \text{(A8)}$$

Note that assuming the Henry's equilibrium for Br_2 in Eq. (A6) and neglecting also the terms relative to the rain would lead to the same equation.

Supplementary material related to this article is available online at: http://www.atmos-chem-phys-discuss.net/11/29561/2011/ acpd-11-29561-2011-supplement.pdf.

Acknowledgements. This work is supported by the EU project SHIVA (226224-FP7-ENV-2008-1). The numerical simulations were performed on the cluster of the Centre de Calcul Scientifique en Région Centre. CATT-BRAMS is a free software provided by CPTEC/INPE and distributed under the CC-GNU-GPL license. We also thank John Crowley for fruitful discussions on this work.

INSU
Institut national des **sciences** de **l'Univers**

The publication of this article is financed by CNRS-INSU.

References

Arteta, J., Marécal, V., and Rivière, E. D.: Regional modelling of tracer transport by tropical convection – Part 1: Sensitivity to convection parameterization, Atmos. Chem. Phys., 9, 7081–7100, doi:10.5194/acp-9-7081-2009, 2009.

Audiffren, N., Renard, M., Buisson, E., and Chaumerliac, N.: Deviations from the Henry's law equilibrium during cloud events: a numerical approach of the mass transfer between phases and its specific numerical effects, Atmos. Res., 49, 139–161, 1998.

Aschmann, J., Sinnhuber, B.-M., Atlas, E. L., and Schauffler, S. M.: Modeling the transport of very short-lived substances into the tropical upper troposphere and lower stratosphere, Atmos. Chem. Phys., 9, 9237–9247, doi:10.5194/acp-9-9237-2009, 2009.

Aschmann, J., Sinnhuber, B.-M., Chipperfield, M. P., and Hossaini, R.: Impact of deep convection and dehydration on bromine loading in the upper troposphere and lower stratosphere, Atmos. Chem. Phys., 11, 2671–2687, doi:10.5194/acp-11-2671-2011, 2011.

Barrie, L. A., Bottenheim, J. W., Schnell, R. C., Crutzen, P. J., Rasmussen, R. A.: Ozone destruction and photochemical reactions at polar sunrise in the lower arctic atmosphere, Nature, 334, 138–141, 1988.

Barth, M. C., Stuart, A. L., and Skamarock, W. C.: Numerical simulations of the July 10,1996, Stratospheric-Tropospheric experiment: radiation, aerosols and ozone (STERAO)-deep convection experiment storm: redistribution of soluble tracers, J. Geophys. Res., 106, 12381–12400, 2001.

Barth, M. C., Sillman, S., Hudman, R., Jacobson, M. Z., Kim, C.-H., Monod, A., and Liang, J.: Summary of the cloud chemistry modelling intercomparison: photochemical box model simulation, J. Geophys. Res., 108(D7), 4214, doi:10.1029/2002JD002673, 2003.

Barth, M. C., Kim, S.-W., Skamarock, W. C., Stuart, A. L., Pickering, K. E., Ott, L. E.: Simulations of the redistribution of formaldehyde, fomic acid, and peroxides in the July 1996 stratospheric-tropospheric experiment: radiation, aerosols and ozone deep convection storm, J. Geophys. Res., 112, D13310, doi:10.1029/2006JD008046, 2007.

Bobrowski, N., von Glasow, R., Aiuppa, A., Inguagiatte, S., Louban, I., Ibrahim, O. W., Platt. U.: Reactive halogen chemistry in volcanic plumes, J. Geophys. Res., 112, D06311, doi:10.1029/2006JD007206, 2007.

Bousserez, N., Attié, J.-L., Peuch, V.-H., Michou, M., Pfister, G., Edwards, D., Avery, M., Sachse, G., Browell, E., and Ferrare, E.: Evaluation of MOCAGE chemistry and transport model during the ICARTT/ITOP experiment, J. Geophys. Res., 112, D120S42, doi:10.1029/2006JD007595, 2007.

Brioude, J., Portmann, R. W., Daniel, J. S., Cooper, O. R., Frost, G. J., Rosenlof, K. H., Granier, C., Ravishankara, A. R., Montkza, S. A., and Sthol, A.: Variations in ozone depletion potentials of very short-lived substances with season and emission region, Geophys. Res. Lett., 37, L19804, doi:10.1029/2010GL044856, 2010.

Dorf, M., Butz, A., Camy-Peyret, C., Chipperfield, M. P., Kritten, L., and Pfeilsticker, K.: Bromine in the tropical troposphere and stratosphere as derived from balloon-borne BrO observations, Atmos. Chem. Phys., 8, 7265–7271, doi:10.5194/acp-8-7265-2008, 2008.

Gettelmann, A., Lauritzen, P. H., Park, M., and Kay, J. E.: Processes regulating short-lived species in the tropical tropopause layer, J. Geophys. Res., 114, D13303, doi:10.1029/2009JD011785, 2009.

Fickert, S., Adams, J. W., and Crowley, J. N.: Activation of Br_2 and BrCl via uptake of HOBr onto aqueous salt solutions, J. Geophys. Res., 104, 23719–23727, 1999.

Freitas, S. R., Longo, K. M., Silva Dias, M. A. F., Chatfield, R., Silva Dias, P., Artaxo, P., Andreae, M. O., Grell, G., Rodrigues, L. F., Fazenda, A., and Panetta, J.: The Coupled Aerosol and Tracer Transport model to the Brazilian developments on the Regional Atmospheric Modeling System (CATT-BRAMS) – Part 1: Model description and evaluation, Atmos. Chem. Phys., 9, 2843–2861, doi:10.5194/acp-9-2843-2009, 2009.

Fueglistaler, S., Dessler, A. E., Dunkerton, T. J., Folkins, I., Fu, Q., and Mote, P. W.: Tropical tropopause layer, Rev. Geophys., 47, RG1004, doi:10.1029/2008RG000267, 2009.

Hossaini, R., Chipperfield, M. P., Monge-Sanz, B. M., Richards, N. A. D., Atlas, E., and Blake, D. R.: Bromoform and dibromomethane in the tropics: a 3-D model study of chemistry and transport, Atmos. Chem. Phys., 10, 719–735, doi:10.5194/acp-10-719-2010, 2010.

Hoyle, C. R., Marécal, V., Russo, M. R., Allen, G., Arteta, J., Chemel, C., Chipperfield, M. P., D'Amato, F., Dessens, O., Feng, W., Hamilton, J. F., Harris, N. R. P., Hosking, J. S., Lewis, A. C., Morgenstern, O., Peter, T., Pyle, J. A., Reddmann, T., Richards, N. A. D., Telford, P. J., Tian, W., Viciani, S., Volz-Thomas, A., Wild, O., Yang, X., and Zeng, G.: Representation of tropical deep convection in atmospheric models – Part 2: Tracer transport, Atmos. Chem. Phys., 11, 8103–8131, doi:10.5194/acp-11-8103-2011, 2011.

Jaeglé, L., Jacob, D. J., Brune, W. H., and Wennberg, P. O.: Chemistry of HO_x radicals in the upper troposphere, Atmos. Environ., 35, 469–489, 2001.

Josse, B., Simon, P., and Peuch, V.-H. : Radon global simulations with the multiscale chemistry and transport model MOCAG E, Tellus B, 56, 339–356, 2004.

Lefèvre, F., Brasseur, G. P., Folkins, I., Smith, A. K., and Simon, P.: Chemistry of the 1991–1992 stratospheric winter: three-dimensional model simulations, J. Geophys. Res., 99, 8183–8195, 1994.

Krysztofiak, G., Catoire, V., Poulet, G., Marécal, V., Pirre, M., Louis, F., Canneaux, S., and Josse, B.: Detailed modelling of the mechanism of the atmospheric degradation of brominated very-short lived species, to be submitted to Atmos. Environ., 2011.

Mellor, G. and Yamada, T.: Development of a turbulence closure model for geophysical fluid problems, Rev. Geophys., 20, 851–875, 1982.

Meylan W. M. and Howard P. H.: Bond contribution method for estimating Henry's law constants, Environ. Toxicol. Chem., 10, 1283–1293, 1991.

Nirmalakhandan N. N. and Speece R. E.: Prediction of aqueous solubility of organic chemicals based on molecular structure, Environ. Sci. Technol., 22, 328–338, 1988.

Pisso, I., Haynes, P. H., and Law, K. S.: Emission location dependent ozone depletion potentials for very short-lived halogenated species, Atmos. Chem. Phys., 10, 12025–12036, doi:10.5194/acp-10-12025-2010, 2010.

Quack, B. and Wallace, D. W. R.: Air-sea flux of bromoform: controls, rates, and implications, Global Biogeochem. Cy., 17, 1023, doi:10.1029/2002GB001890, 2003.

Roberts, T. J., Braban, C. F., Martin, R. S., Oppenheimer, C., Adams, J. W., Cox, R. A., Jones, R. L., and Griffiths, P. T.: Modelling reactive halogen formation and ozone depletion in volcanic plumes, Chem. Geol., 263, 151–163, 2009.

Sander, R.: Compilation of Henry's Law Constants for Inorganic and Organic Species of Potential Importance in Environmental Chemistry (Version 3), available at: http://www.henrys-law.org (last access: August 2011), 1999.

Sander R. and Crutzen, P. J.: Model study indicating halogen activation and ozone destruction in polluted air mass transported to the sea, J. Geophys. Res., 101, 9121–9138, 1996.

Sandu, A., Verwer, J. G., Blom, J. G., and Spee, E. J.: Benchmarking stiff ode solvers for atmospheric chemistry problems II: Rosenbrock solvers, Atmos. Environ., 31, 3459–3472, 1997.

Schofield, R., Fueglistaler, S., Wohltmann, I., and Rex, M.: Sensitivity of stratospheric Br_y to uncertainties in very short lived substance emissions and atmospheric transport, Atmos. Chem. Phys., 11, 1379–1392, doi:10.5194/acp-11-1379-2011, 2011.

Sinnhuber, B.-M., Rosanov, A., Sheode, N., Afe, O. T., Richter, A., Sinnhuber, M., Wottrock, F., Burrows, J. P., Stiller, G. P., von Clarmann, T., and Linden, A.: Global observations of stratospheric bromine monxide from SCIAMACHY, Geophys. Res. Lett., 32, L20810, doi:10.1029/2005GL023829, 2005.

Stockwell, W. R., Kirchner, F., Kuhn, M., and Seefeld, S.: A new mechanism for regional atmospheric chemistry modeling, J. Geophys. Res., 102, 25847–25879, 1997.

Tie, X., Madronich, S., Walters, S., Zhang, R., Rasch, P., and Collins, W.: Effects of clouds on photolysis and oxidants in the troposphere, J. Geophys. Res., 108, 4642, doi:10.1029/2003JD003659, 2003.

Toon, O. B., McKay, C. P., Ackerman, T. P., and Santhanam, K. L.: Rapid calculation of radiative heating rates and photodisociation rates in inhomogeneous multiple scattering atmospheres, J. Geophys. Res., 94, 16287–16301, 1989.

Von Glasow, R. and Crutzen P. J.: Troposheric Halogen Chemistry, Treatise on Geochemistry Update 1, edited by: Holland, H. D. and Turekian, K. K., vol. 4.02, Elsevier-Pergamon, Oxford, 1–67, 2007.

Walko, R. L., Cotton, W. R., Meyers, M. P., and Harrington, J. Y.: New RAMS cloud microphysics parameterization, Part I: the single-moment scheme, Atmos. Res., 38, 29–62, 1995.

Wesely, M. L.: Parametrization of surface resistances to gaseous dry deposition in regional scale numerical models, Atmos. Environ., 23, 1293–1304, 1989.

World Meteorological Organization: Scientific assessment of ozone depletion, 2006, Global ozone research and monitoring project-report No 50, Geneva, Switzerland, 2007.

Yang, X., Cox, R. A., Warwick, N. J., Pyle, J. A., Carver, G. D., O'Connor, F. M., and Savage N. H.: Tropospheric bromine chemistry and its impact on ozone: a model study, J. Geophys. Res., 110, D23311, doi:10.1029/2005JD006244, 2005.

Yokouchi, Y., Hasebe, F., Fujiwara, M., Takashima, H., Shiotani, M., Nishi, N., Kanaya, Y., Hashimoto, S., Fraser, P., Toom-Sauntry, D., Mukai, H., and Nojiri, Y.: Correlations and emission ratios among bromoform, dibromochloromethane, and dibromomethane in the atmosphere, J. Geophys. Res., 110, D23309, doi:10.1029/2005JD006303, 2005.

Zhang, K., Wan, H., Zhang, M., and Wang, B.: Evaluation of the atmospheric transport in a GCM using radon measurements: sensitivity to cumulus convection parameterization, Atmos. Chem. Phys., 8, 2811–2832, doi:10.5194/acp-8-2811-2008, 2008.

Table 1. Accommodation coefficients and values used in the determination of the effective Henry's constants H_X[a] of bromine species X used in the model.

Species	α[f]	H_{298} (mol l^{-1} atm^{-1})	a_H (K)	K_{298} mol l^{-1}	a_K (K)
HBr	0.2	0.71[d]	10 200.[d]	1×10^{9}[d]	0.[d]
HOBr	0.2	6.1×10^{3}[b]	5900.[c]	0.	0.
Br_2	0.05	0.76[d]	4177.[d]	0.	0.
CBr_3OOH	0.2	1.96×10^{5}[e]	5200.[g]	0.	0.
$CHBr_2OOH$	0.2	2.25×10^{4}[e]	5200.[g]	0.	0.
CHBrO	0.05	74.[e]	5800.[h]	0.	0.
CBr_2O	0.05	21.5[e]	5400.[h]	0.	0.

[a] $H_X = H_{298}\exp\Bigl(a_H\left(\frac{1}{T}-\frac{1}{298}\right)\Bigl(1+\frac{K_{298}}{[H^+]}\Bigr)\exp\left(a_K\left(\frac{1}{T}-\frac{1}{298}\right)\right)\Bigr)\Bigr)$.

[b] Sander (1999).

[c] As for HOCl (Sander, 1999).

[d] Yang et al. (2005).

[e] Krysztofiak et al. (2011).

[f] Barth et al. (2001).

[g] As for CH_3OOH (Sander, 1999).

[h] Mean temperature dependency of RCHO and RR′CO (Sander, 1999).

CC BY

Table 2. Concentration and lifetime of important species for the organic bromine chemistry in the BG simulation.

OH^a (cm^{-3})	$HO_2{}^a$ (cm^{-3})	$NO_x{}^a$ (pptv)	$O_3{}^a$ (ppbv)	O_3 column[a] (DU)	$\tau_{OH}{}^b$ (days)	$\tau_J{}^c$ (days)	τ^d (days)
2.72×10^6	1.96×10^8	13	14	250	22.6	15.2	9.1

[a] Averaged values over the 10 days of the simulation at 1 km altitude.
[b] Lifetime of $CHBr_3$ relative to OH.
[c] Lifetime of $CHBr_3$ relative to photolysis.
[d] Total lifetime of $CHBr_3$.

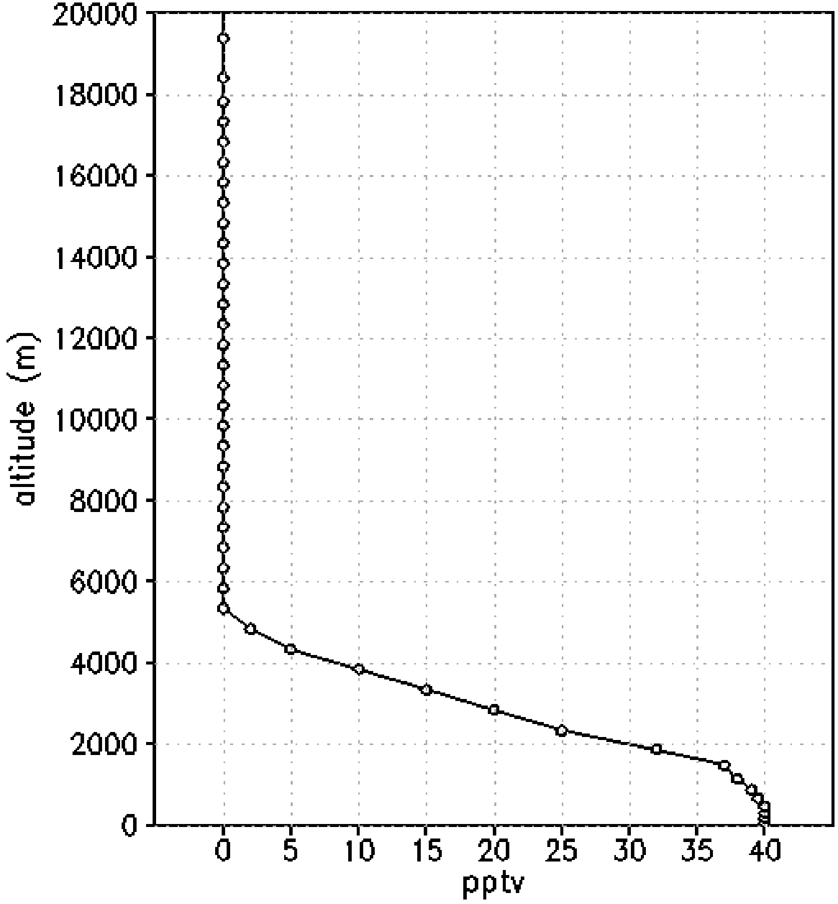

Fig. 1. Initial bromoform profile used in the calculations. This profile is set homogeneously horizontally over the whole domain.

CC BY

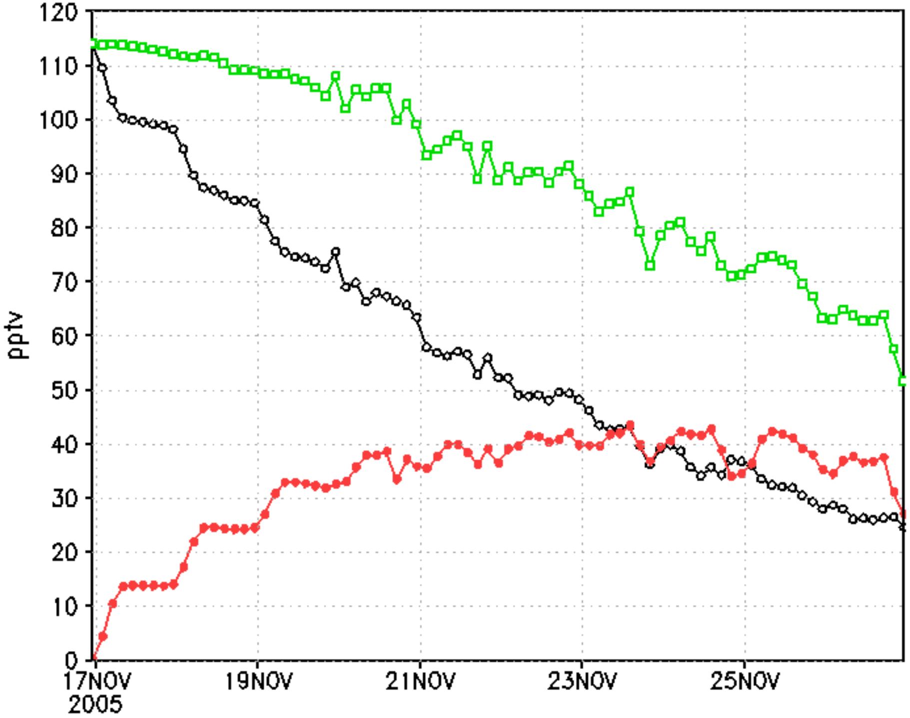

Fig. 2. Time evolution of the mixing ratio of bromine atoms (pptv) in bromoform (black), in product gases (red) and in the sum (green) over the 10 days of the BG simulation at 1 km altitude 12.4° S and 130°9 W (middle point of the domain).

cc BY

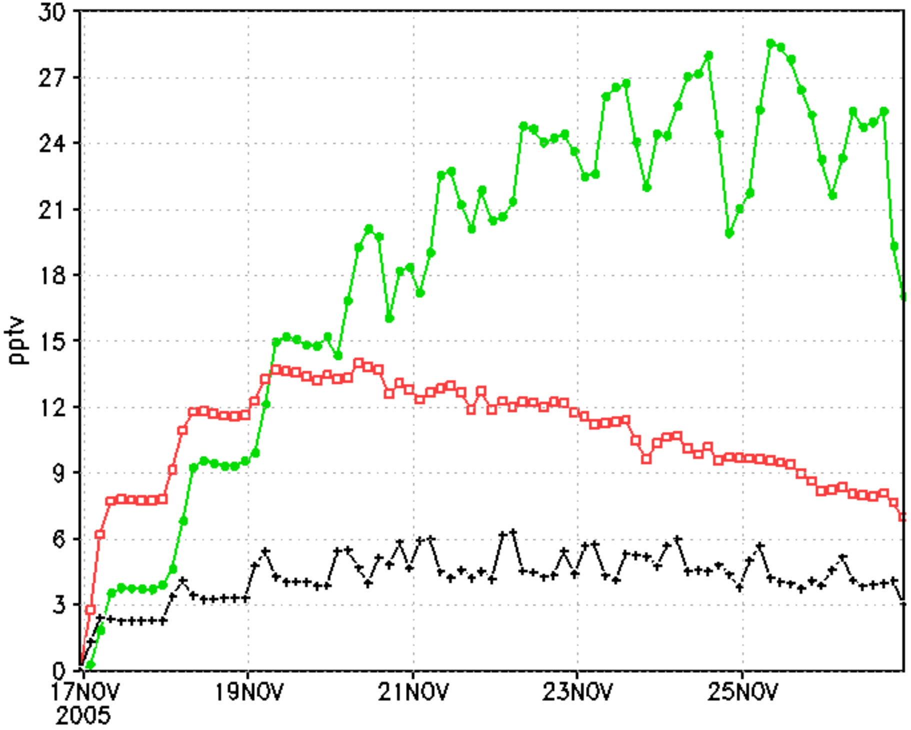

Fig. 3. Same as Fig. 2 but for HBr (green), for organic products ($CBr_3OOH + CHBr_2OOH + CBr_2O + CHBrO$) (red) and for other inorganic products ($Br + BrO + HOBr + BrONO_2$) (black).

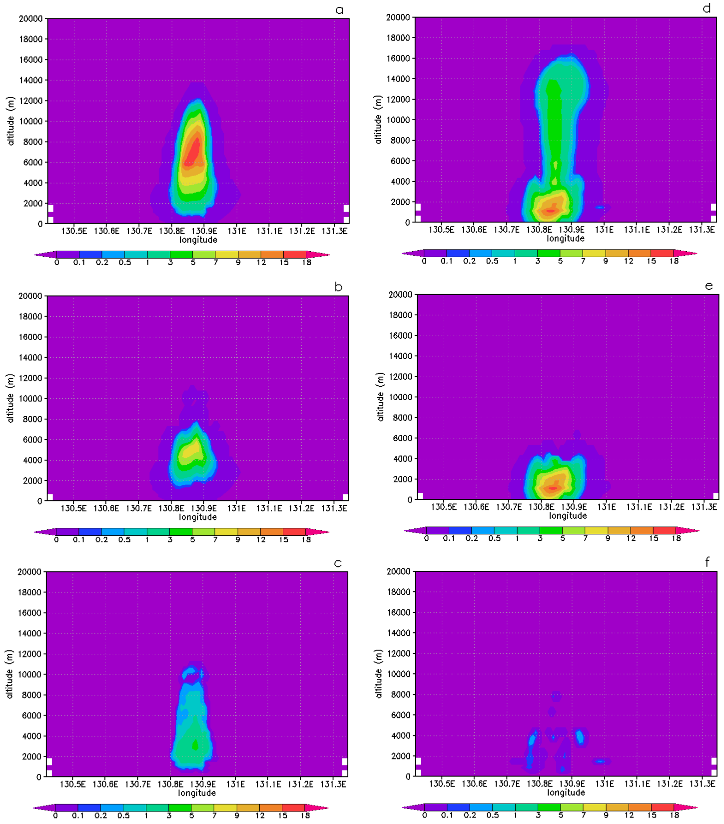

Fig. 4. Longitude-altitude cross section at 12.4° S of **(a)** the total condensed water (liquid + ice) mixing ratio (g kg^{-1}) at t_0 + 20 min, **(b)** the rain mixing ratio (g kg^{-1}) at t_0 + 20 min, **(c)** the liquid cloud mixing ratio (g kg^{-1}) at t_0 + 20 min, **(d)** the total condensed water (liquid + ice) mixing ratio at t_0 + 30 min, **(e)** the rain mixing ratio (g kg^{-1}) at t_0 + 30 min and **(f)** the liquid cloud mixing ratio at t_0 + 30 min. t_0 is 5 days and 6 h after the beginning of the simulation.

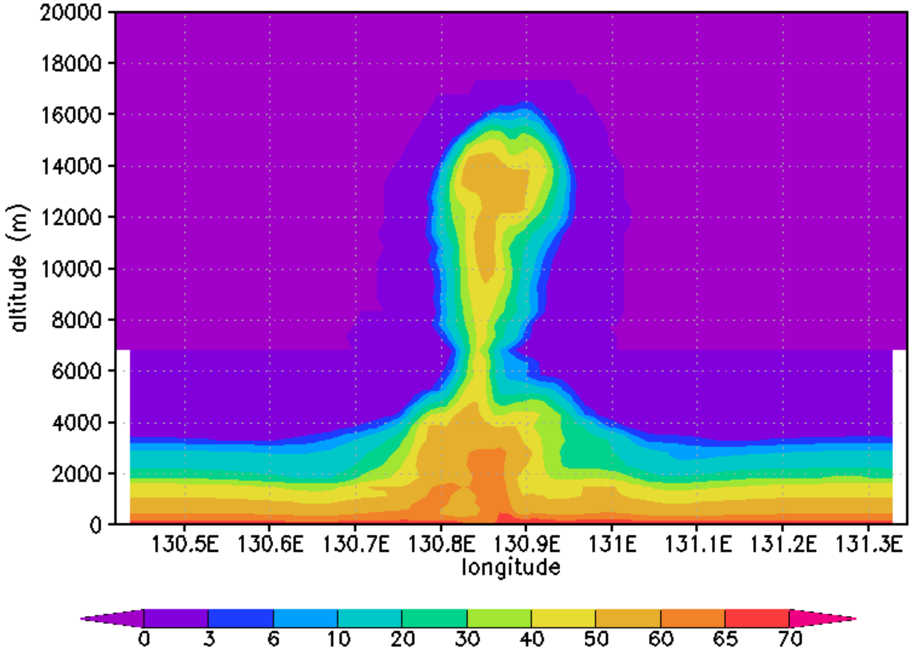

Fig. 5. Longitude altitude cross-section of the mixing ratio (pptv) of bromine atoms in $CHBr_3$ at 12.4° S at $t_0 + 30$ min.

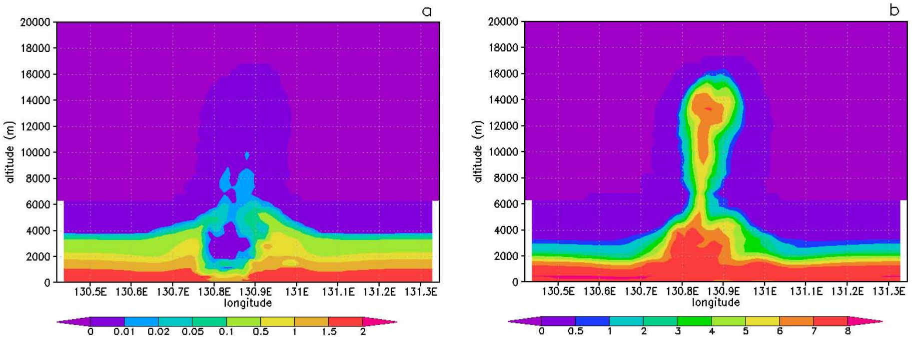

Fig. 6. Longitude-altitude cross-section at 12.4° S at $t_0 + 30$ min of the mixing ratio (pptv) of bromine atoms in **(a)** CBr_3OOH and **(b)** CBr_2O.

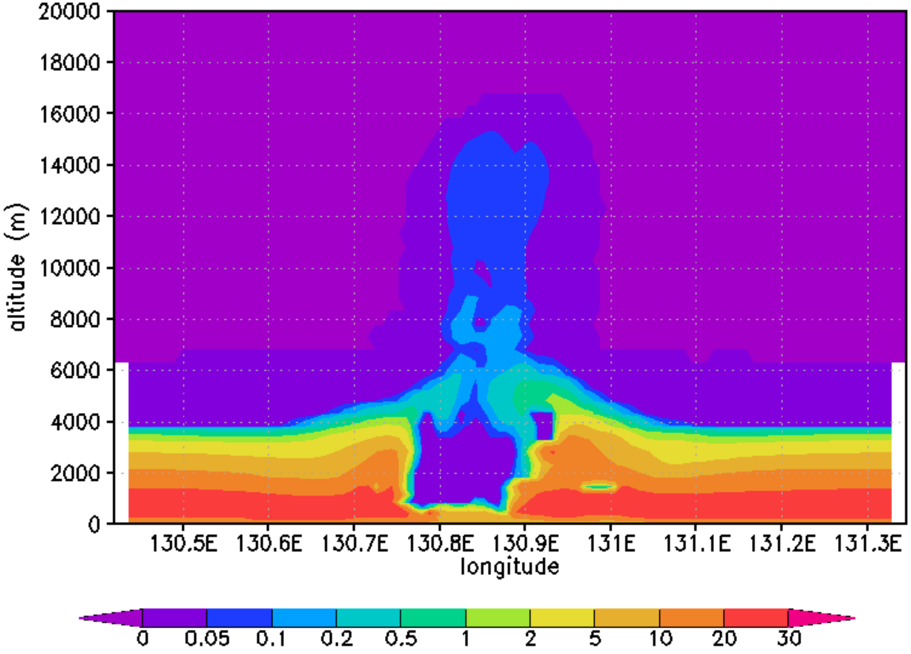

Fig. 7. Longitude-altitude cross section at 12.4° S at $t_0 + 30$ min of HBr in pptv.

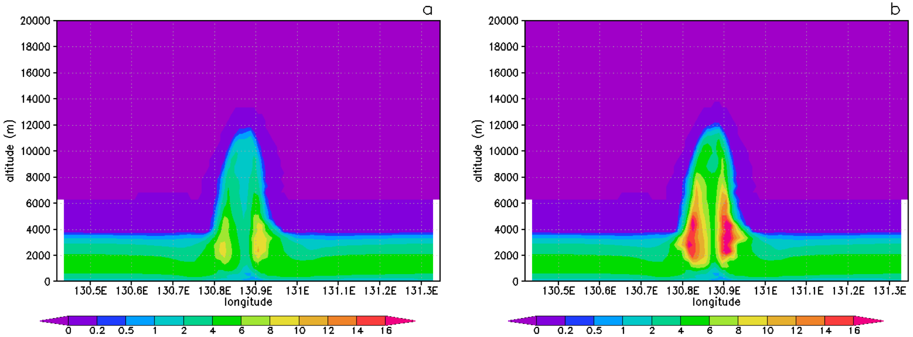

Fig. 8. Longitude-altitude cross section at 12.4° S at t_0+20 min of $Br_x=Br+BrO+2\cdot Br_2+HOBr$ in pptv for **(a)** cloud pH = 5 and **(b)** cloud pH = 4.

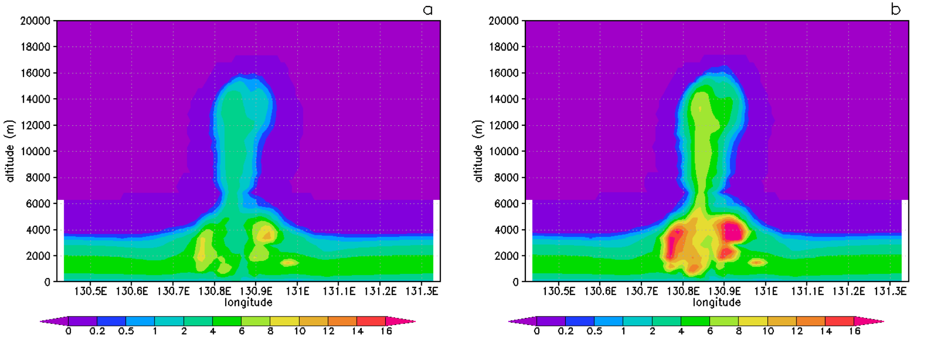

Fig. 9. Same as Fig. 8 but for $t_0 + 30$ min.

Title Page
Abstract | Introduction
Conclusions | References
Tables | Figures
◀| |▶
◀ ▶
Back | Close
Full Screen / Esc
Printer-friendly Version
Interactive Discussion

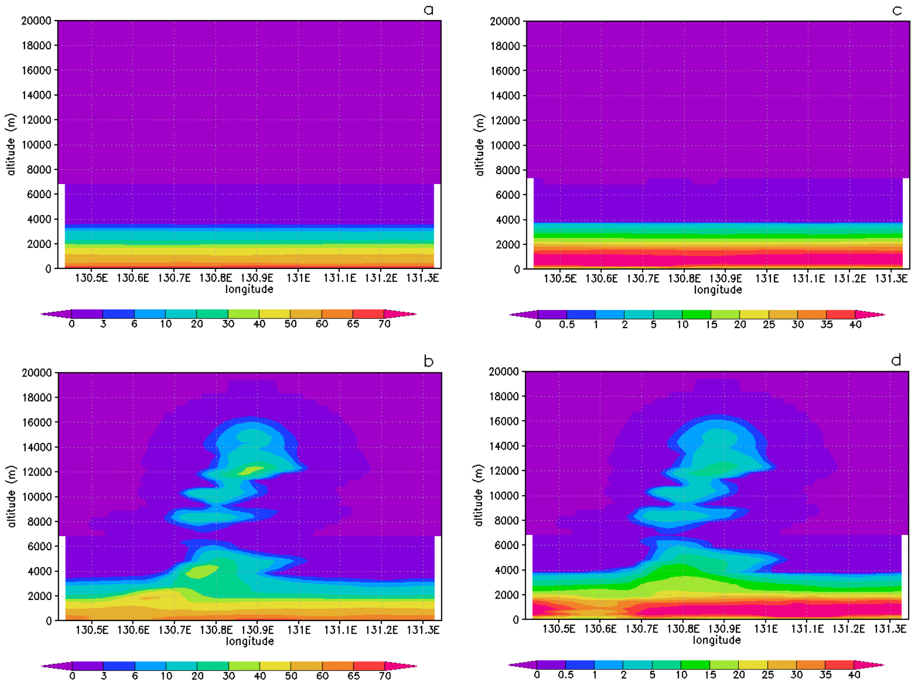

Fig. 10. Longitude-altitude cross section at 12.4° S of bromine atoms for cloud pH = 5 in at $t_0 + 110$ min in **(a)** $CHBr_3$ in the BG simulation, **(b)** $CHBr_3$in the PERT simulation, **(c)** total PGs in the BG simulation, **(d)** total PGs in the PERT simulation.

Title Page
Abstract | Introduction
Conclusions | References
Tables | Figures
◀| |▶
◀ ▶
Back | Close
Full Screen / Esc
Printer-friendly Version
Interactive Discussion

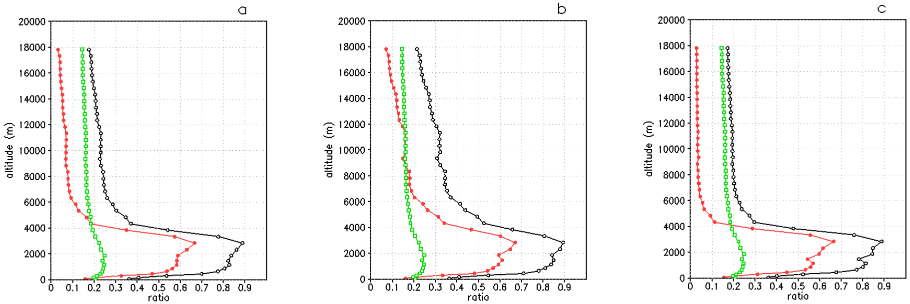

Fig. 11. Mean profile at the end of the convective event ($t_0 + 110$ min) of the ratio of the bromine atoms mixing ratio in the total PGs over the bromine atoms mixing ratio in $CHBr_3$ averaged on the horizontal (black); same for inorganic PGs over $CHBr_3$ (red); same for organic PGs over $CHBr_3$ (green) **(a)** for cloud pH = 5, **(b)** for cloud pH = 4 and **(c)** if the hydrolysis of $BrONO_2$ and the reactions in aqueous phase of HBr, HOBr and Br_2 are not taken into account in the simulations.